IEEE Access
Multidisciplinary | Rapid Review | Open Access Journal

Received December 16, 2020, accepted December 30, 2020, date of publication January 1, 2021, date of current version January 12, 2021.

*Digital Object Identifier 10.1109/ACCESS.2020.3048783*

# A Novel Energy Management Strategy Design Methodology of a PHEV Based on Data-Driven Approach and Online Signal Analysis

**JIANAN ZHANG, LIANG CHU, CHONG GUO, ZICHENG FU, AND DI ZHAO**
College of Automotive Engineering, Jilin university, Changchun 130025, China

Corresponding author: Chong Guo (guochong@jlu.edu.cn)

This work was supported in part by the Outstanding Young Talents Foundation of Jilin Province (CN) under Grant 20190103160JH, and in part by the Science and Technology Program of Tianjin (CN) under Grant 20YFZCGX00770.

**ABSTRACT** This paper introduces an energy management strategy design method for a plug-in hybrid electric vehicle based on the data-driven approach and online signal analysis. It includes two parts, mode division strategy design, and power distribution strategy design. Using the random forest in data mining technology to analyze optimization results of dynamic programming can quickly extract key information and establish optimal and understandable mode division strategy with high precision and stability directly. Besides, integrating the classic ''Engine optimal operating curve control'' strategy with wavelet transform and Markov prediction, which not only enhances the adaptability of the strategy to different driving conditions but also improves the fuel economy by reducing the impact of transient power on the engine operation. At the same time, to improve the prediction accuracy of the algorithm without increasing the computational complexity, this paper adds a prediction result correction function to the first-order Markov prediction model to reduce the impact of slow update of the probability matrix on prediction accuracy. The simulation results show the average prediction error of the improved Markov prediction model is reduced by 5.3% and the new energy management strategy designed reduces fuel consumption by 8.28% at the cost of a small increase in electricity consumption.

**INDEX TERMS** Plug-in hybrid electric vehicle, dynamic programming, random forest, Markov chain, wavelet transform.

## I. INTRODUCTION

Compared with petrol energy vehicles, new energy vehicles have advantages in fuel consumption and emission. As one of the measures to improve vehicle fuel economy, energy management strategy (EMS) has always been a research hotspot in industry and academia [1]–[3].

### A. LITERATURE REVIEW

Existing EMS can be generally classified into rule-based and optimization-based strategies [4]–[6]. Rule-based strategies (RBS) can be constructed by mathematical models or engineering expertise, which have short computing time, high reliability, and easy implementation. However, despite extensive experimentation and calibration work, their optimality and adaptability may still not be guaranteed [7]–[9]. Optimization-based strategies (OBS) generally calculate (near) optimal results by using a strategy that minimizes the sum of objective functions over time (global optimization) or by instantly minimizing an objective function (local optimization). However, they can hardly be applied in real-time for the high dependency on driving cycles or online computational complexity [10]–[13]. To find a better trade-off technique to compromise optimization and computation load, a feasible solution is presented in this paper. First, the data-driven method is used offline to obtain optimal RBS. Then the power distribution strategy is adjusted online according to different driving conditions through short-term velocity prediction and power demand signal analysis.

According to the practicability of the RBS, some studies focus on the optimization of the RBS to improve the

The associate editor coordinating the review of this manuscript and approving it for publication was Yang Tang.

fuel economy [14]. Such as Peng *et al.* in [15], Lei *et al.* in [16], Wang *et al.* in [17], Zhou *et al.* in [18]. Using optimization-based methods to improve the fixed control rules not only has a good performance in terms of energy consumption improvement but also saves a lot of calibration work. Among these optimization methods, dynamic programming (DP) is a well-known optimization method based on Bellman's principle of optimality [19], which outperforms many other optimization methods due to its ability to acquire the global optimal solution based on receding cost minimization [20]–[23]. Therefore, to ensure optimality, it is a suitable choice to extract RBS from the DP optimization results.

To improve the adaptability of the extracted rules, as many DP results as possible are needed to support them. Therefore, the analysis and extraction work of large amounts of data cannot only rely on manpower but need to use machine learning (ML) methods. The decision tree (DT) is a widely used ML technique for classification and regression purposes. Knowledge gathered by DT is not only understandable by humans but also can be converted into a sequence of rules which can readily be implemented in embedded systems [24], [25]. While random forest (RF) is an integrated learning method that is operated by constructing a multitude of DTs at training time and outputting the classification results that are averaged or voted by every individual tree [26], which can reduce the error that may occur when specific DT is over-fitting and improve the accuracy of the model [27]–[30]. Therefore, this paper will apply RF to design RBS based on the classification and regression of DP optimization results.

Due to the influence of complex and changeable traffic environments, the power demand of powertrain usually contains peak power and high transient power, which may cause engine frequent start and stop or insufficient combustion, in turn, leads to deterioration of fuel consumption and vibration issues [31], [32]. An effective solution is to distribute the transient and rapid variations components of power demand to the motor and distribute steady-state power to the engine. This is where the wavelet transform (WT) can provide a potential solution. The WT is a powerful tool for the information analysis of a time series signal, simultaneously in time and frequency domains, which can effectively extract dynamic information from the signal [33]. It has been used in EMS recently for its excellent performance in transient power recognition [34]–[36].

To obtain the power signal to be analyzed in advance, it is necessary to perform short-term prediction. Markov chain (MC) models are well-suited to represent the uncertainty in velocity, power demand... etc., which can lower both the information required for implementation and the on-board computing burden [37], [38]. To improve the prediction accuracy of the MC, some papers use the second-order or even higher-order Markov algorithm [39], [40], but the calculation amount of the algorithms will double or many times. Some papers propose online self-learning MC, such as adding forgetting factors and weight coefficients [41], [42], or combining MC with other advanced algorithms such as Monte Carlo Method [43]. Although good forecasting results have been achieved, these methods still inevitably bring about an increase in the amount of calculation. Therefore, to improve the prediction accuracy while also reducing the computational complexity of the algorithm, this paper proposes an adaptive MC by introducing a prediction result correction function based on the first-order Markov prediction model.

### B. MOTIVATION AND INNOVATION

Therefore, based on the above reasons, this paper proposes a novel energy management strategy design methodology for EMS of a series-parallel plug-in hybrid electric vehicle (PHEV) based on machine learning and online signal analysis. This method can not only ensure the approximate optimality of the formulated rules but also improve their adaptability to different driving conditions.

Fig. 1 is an introduction to the overall idea of the paper. First, use the RF to analyze the optimization results of DP, and get the optimal mode division strategy. The ''Driving data at the $k$th step'' in the figure mainly refers to the velocity, power demand, and SoC at the $k$th step. The information is used to determine the optimal working mode of the $k$th step. After the mode is determined, decide how to allocate the power. Power distribution needs to distinguish between steady-state

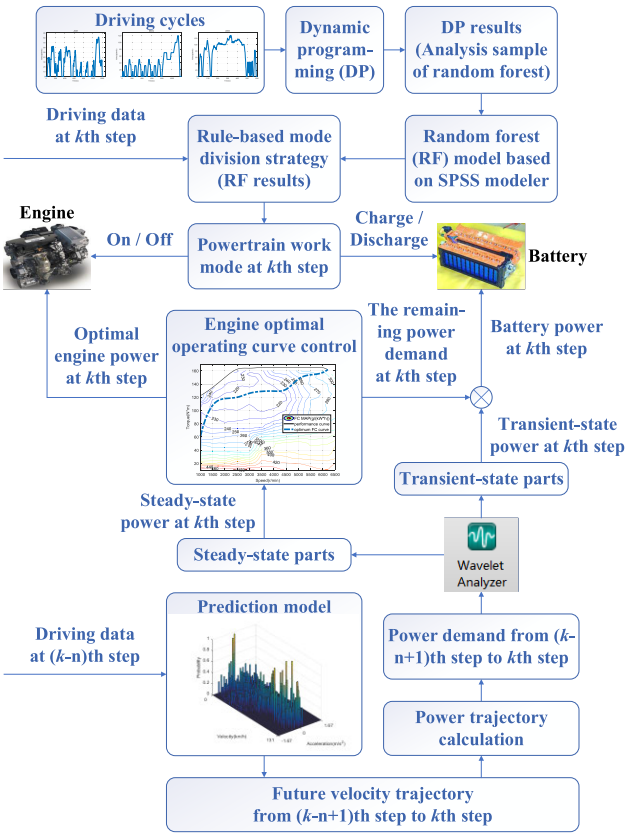


**FIGURE 1.** Overall flowchart about the proposed method.

components and transient components in the power demand through WT. The WT requires that the signal must be known in prior. Therefore, if we want to perform power allocation at the $k$th step, we need to obtain the power demand change trajectory containing the power demand of the $k$th step in advance. Markov prediction is used here. Before the $k$th step is reached, we use the velocity of a certain step (that is, "$(k-n)$th step" in the figure) to predict the velocity of the next few steps (that is, "$(k-n+1)$th step to kth step" in the figure), and obtain the power demand change trajectory of these steps through calculation. Then we can use WT to process the power demand change trajectory.

Compared with existing research, this work provides the following contributions:

1) A mode division strategy design method is proposed by utilizing the random forest model to analyze the optimization results of dynamic programming. In this manner, key information can be quickly extracted and an understandable optimal mode division strategy with high precision and stability is directly established.

2) An improved first-order Markov prediction model is proposed by adding a prediction result correction function, not only reducing the impact of the slow update of the probability matrix on prediction accuracy but also not increasing the complexity of the algorithm.

3) The classic "Engine optimal operating curve control" strategy is improved by integrating with wavelet transform and Markov prediction, which not only enhances the adaptability to different driving conditions but also improves the fuel economy by reducing the impact of transient power on engine operation.

### C. ORGANIZATION

The remainder of this paper is organized as follows: Section II introduces the model of targeted series-parallel PHEV. Section III describes the working mode division strategy design method. Section IV presents the power distribution strategy design method. Section V introduces the verification and discussion. Finally, conclusions are drawn in Section VI.

## II. PLUG-IN HYBRID POWERTRAIN MODEL

The powertrain architecture of the vehicle is shown in Fig. 2. It is a series-parallel PHEV from Honda. Parameters of the PHEV are specified in Table 1.

According to benchmarking test results, the powertrain can operate in six modes: EV mode (pure electric mode) in Charge Depleting (CD) state/Charge Sustaining (CS) state, Hybrid mode (series mode) in CD/CS state, and Engine mode (parallel mode) in CD/CS state. When SoC is lower than 28%, the engine starts and drives the generator to charge the battery, and the powertrain enters the CS state. When the SoC reaches 35%, charging stops and the powertrain enters the CD state. The working mode division of CD state and CS state are shown in Fig. 3 and Fig. 4. The points in the figure represent the working status of the powertrain. For example, in the CD state, when the velocity is 20km/h and the driving force is 6000N, the powertrain works in EV mode. If in the CS state, when the velocity is 20km/h and the driving force is 6000N, the powertrain works in Hybrid mode.

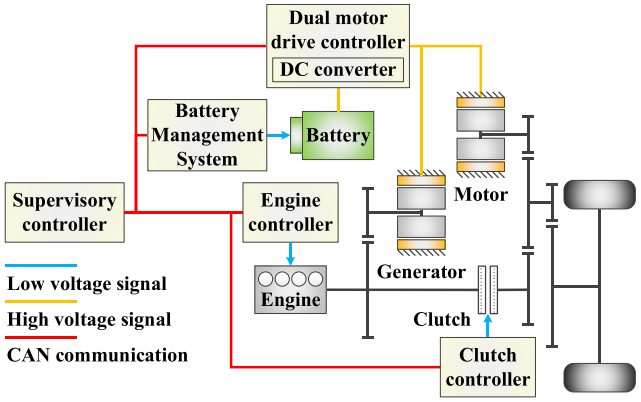


**FIGURE 2.** Powertrain architecture of the vehicle.

**TABLE 1.** Basic parameters of the vehicle and powertrain.

| Parameter | Unit | Value |
|---|---|---|
| Curb mass | kg | 1700 |
| Engine model | - | DOHC Atkinson |
| Engine type | - | Inline 4-cylinder |
| Engine capacity | mL | 1993 |
| Maximum engine power | kW@rpm | 105@6200 |
| Maximum engine torque | Nm@rpm | 165@2500-6000 |
| Maximum motor power | kW | 124 |
| Maximum motor torque | Nm | 307 |
| Maximum motor speed | rpm | 12584 |
| Battery model | - | Lithium ion |
| Battery capacity | kWh | 6.7 |
| Rated battery voltage | V | 300 |
| Engine-generator gear ratio | - | 1.934 |
| Engine-main reducing gear ratio | - | 0.803 |
| Motor-main reducing gear ratio | - | 2.45 |
| Main reducing gear ratio | - | 3.421 |

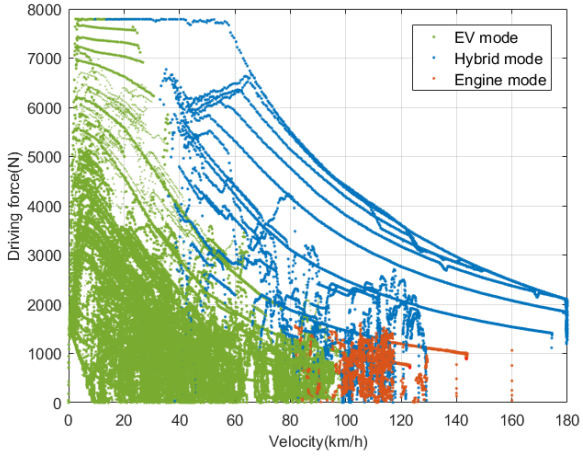


**FIGURE 3.** Working mode division in CD state.

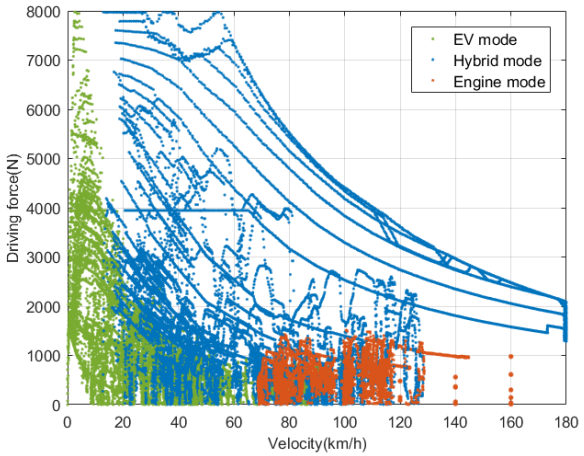


**FIGURE 4.** Working mode division in CS state.

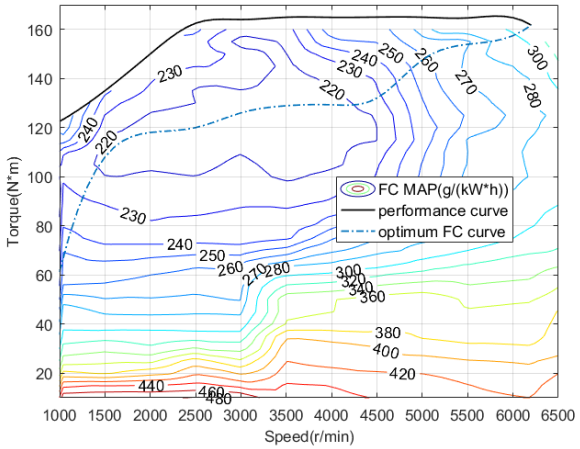


**FIGURE 5.** The engine fuel consumption map.

### A. THE VEHICLE MODEL

The longitudinal driving dynamics equation of the vehicle is expressed by:

$$F_d = F_f + F_w + F_i + F_j = mgf \cdot \cos\alpha + \frac{1}{2}C_D\rho A \cdot v^2 + mg \cdot \sin\alpha + \delta m \cdot a \quad (1)$$

The slope $\alpha$ of the working condition in the model is adjustable, but the main purpose of this paper is to verify the effectiveness of the EMS design method. Therefore, to facilitate analysis, $\alpha$ is set to 0 in the following content.

The acceleration of the vehicle in simulation at $k$th step can be obtained by:

$$a_k = \frac{dv}{dt} = \frac{v_{k+1} - v_k}{t_{k+1} - t_k} \quad (2)$$

The sliding resistance coefficients $A_{dyno}$, $B_{dyno}$, and $C_{dyno}$ of the test vehicle were measured through the sliding test. Therefore, the vehicle torque demand $T_d$ of $k$th step can be expressed as:

$$T_{d\_k} \cdot \eta_{T\_k} = \left(A_{dyno} + B_{dyno} \cdot v_k + C_{dyno} \cdot v_k^2 + \delta m \cdot a_k\right) \cdot r \quad (3)$$

where $\eta_{T\_k}$ is transmission efficiency and $r$ is the rolling radius of the tire.

### B. THE ENGINE MODEL

We build a quasi-static model of the engine system based on experimental data. The fuel consumption can be obtained through the speed and torque look-up table. Therefore, the engine fuel consumption rate $g_e(n_e, T_e)$ at the operating point $(n_e, T_e)$ is obtained from the interpolation function:

$$g_e(n_e, T_e) = f(n_e, T_e) \quad (4)$$

Fig. 5 shows the fuel consumption map of a 2.0L gasoline engine.

### C. THE GENERATOR AND MOTOR MODELS

The experimental modeling method is also used to develop the generator model and the motor model. According to the literature, the generator and motor have the same motor specifications. Their efficiency can be obtained from the speed and torque look-up table. Fig. 6 is the generator/motor efficiency map. The generator efficiency $\eta_{gen}(n_{gen}, T_{gen})$ at the operating point $(n_{gen}, T_{gen})$ is obtained from the following interpolation function:

$$\eta_{gen}\left(n_{gen}, T_{gen}\right) = f(n_{gen}, T_{gen}) \quad (5)$$

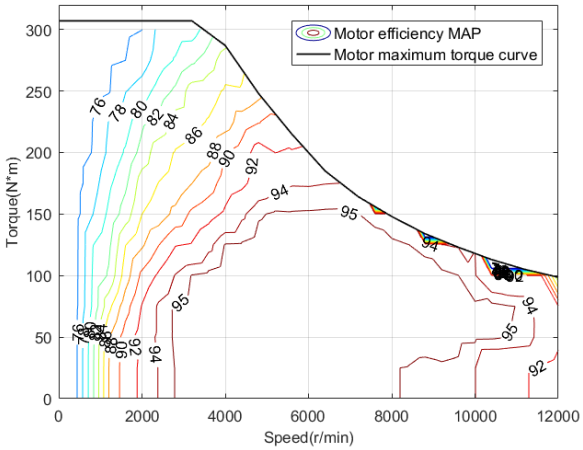


**FIGURE 6.** The generator/motor efficiency map.

And the motor is the same:

$$\eta_{mot}\left(n_{mot}, T_{mot}\right) = f(n_{mot}, T_{mot}) \quad (6)$$

### D. THE BATTERY MODEL

The experimental modeling method is also used to develop the battery model. A lithium battery is used in the test vehicle. Rint model is commonly used in describing the characteristics of the lithium battery, which is applied because of its simplicity and little inaccuracy. This model is illustrated

in Fig. 7. And Equation (7) can demonstrate the mathematical character of the battery:

$$P_{bat} = U \cdot I = (U_{oc} - I \cdot R_{int}) \cdot I = U_{oc} \cdot I - I^2 \cdot R_{int} \quad (7)$$

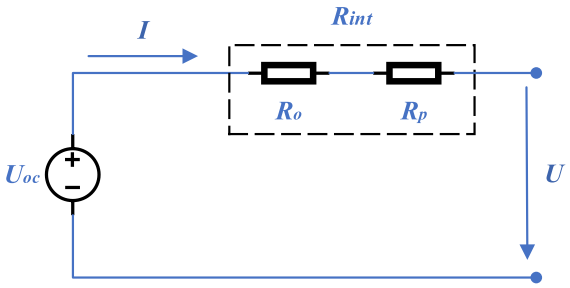


**FIGURE 7.** The rint battery model.

where $U_{oc}$ is the battery open-loop voltage, which can be obtained from the battery temperature and battery SoC look-up table based on test data. $R_{int}$ is the battery internal resistance, including ohmic resistance $R_o$ and polarization resistance $R_p$, which can also be obtained from the battery temperature and battery SoC look-up table based on test data.

Determined by generator power and motor power, $P_{bat}$ can also be expressed by:

$$P_{bat} = sgn(P_{gen}) \cdot P_{gen} \cdot \eta_{gen}^{-sgn(P_{gen})} + sgn(P_{mot}) \cdot P_{mot} \cdot \eta_{mot}^{-sgn(P_{mot})} \quad (8)$$

where $sgn(P_{gen})$ and $sgn(P_{mot})$ represent the working states of the generator and motor, the value is 1 when driving, and the value is $-1$ when generating electricity.

For the convenience of calculations, Equation (7) is transformed into the following form:

$$I = \frac{U_{oc} - \sqrt{U_{oc}^2 - 4R_{int} \cdot P_{bat}}}{2R_{int}} \quad (9)$$

So the change rate of the battery SoC can be obtained by:

$$\frac{dSoC}{dt} = -\frac{I}{C} = -\frac{U_{oc} - \sqrt{U_{oc}^2 - 4R_{int} \cdot P_{bat}}}{2R_{int} \cdot C} \quad (10)$$

where $C$ is the battery capacity.

Transform Equation (10) to a discrete form, and battery SoC at the $k$th step is obtained:

$$SoC_k = SoC_{k-1} - \frac{U_{oc\_k-1} - \sqrt{U_{oc\_k-1}^2 - 4R_{int\_k-1} \cdot P_{bat\_k-1}}}{2R_{int\_k-1} \cdot C} \quad (11)$$

## III. MODE DIVISION STRATEGY DESIGN

With multiple energy sources and power components, the plug-in hybrid electric vehicle can flexibly switch working modes to achieve the finest performance and minimum energy consumption. The commonly used method in engineering is to calculate the comprehensive efficiency of each mode of the powertrain first and determine the work ranges of different modes by projecting the efficiency surface to the velocity-power demand plane. It is a simple and effective method. The target PHEV is a typical application example of this kind of strategy. However, only the characteristics of the components are considered, while the influence of driving conditions is ignored, so it is difficult to achieve the lowest fuel consumption. The popular method in papers is generally to combine intelligent algorithms and optimization algorithms, which not only ensures optimality but also improves the adaptability of the strategy to different driving conditions. However, they can hardly be applied in real-time for the high dependency on driving cycles or online computational complexity. Therefore, this paper decides to find control laws through offline analysis of a large number of optimal control results of dynamic programming utilizing a data-driven method, to formulate a rule-based mode division strategy that is easy to implement online.

### A. DYNAMIC PROGRAMMING

The basic idea of DP is to disassemble a complex problem that requires multiple decisions into multiple related simple problems and solve each simple problem recursively to achieve the optimization of complex multi-stage decision-making problems. The establishment of the DP model requires the completion of the following tasks:

#### 1) IDENTIFY THE PROBLEMS TO BE OPTIMIZED AND DIVIDE THE OPTIMIZATION PROCESS INTO STAGES

In comparison with fuel consumption, electricity consumption has the advantages of low price and zero-emission when used to drive the same distance [44]. Thus, the optimization goal is to minimize fuel consumption by consuming electric power until the PHEV reaches the destination. To find a better trade-off scheme to compromise calculation accuracy and model complexity, each second in the driving cycle is regarded as a stage of the optimization process. And the objective function can be obtained:

$$J_k = \begin{cases} \min\ (\dot{m}_{f\_k} + J_{k+1}), & k = 0, 1, \ldots, R-2, R-1 \\ 0, & k = R \end{cases} \quad (12)$$

where $J_k$ is the total fuel consumption at $k$th step and $\dot{m}_{f\_k}$ is the fuel consumption rate at $k$th step. $R$ is a positive integer which represents the duration of the driving cycle.

#### 2) DETERMINE STATE VARIABLES, CONTROL VARIABLES AND STATE TRANSITION FUNCTION

In this paper, battery $SoC_k$ is taken as the state variable and motor torque $T_{mot\_k}$, engine speed $n_{e\_k}$ and engine torque $T_{e\_k}$ are taken as the control variables. And the state transition function of the PHEV model can be expressed by the

following equation:

$$\begin{cases} x_{k+1} = f(x_k, u_k) \\ x = SoC_k \\ u = [T_{mot\_k} n_{e\_k} T_{e\_k}] \end{cases} \tag{13}$$

#### 3) DETERMINE THE CONSTRAINTS

During the optimization, it is necessary to impose certain inequality constraints to ensure safe/smooth operation of the components and driver's demand can be met, so the boundary conditions are as follows:

$$\begin{cases} SoC_{min} \le SoC_k \le SoC_{max} \\ n_{e\_min} \le n_{e\_k} \le n_{e\_max} \\ T_{e\_min}(n_{e\_k}) \le T_{e\_k} \le T_{e\_max}(n_{e\_k}) \\ n_{gen\_min} \le n_{gen\_k} \le n_{gen\_max} \\ T_{gen\_min}(n_{gen\_k}, SoC_k) \le T_{gen\_k} \le T_{gen\_max}(n_{gen\_k}, SoC_k) \\ n_{mot\_min} \le n_{mot\_k} \le n_{mot\_max} \\ T_{mot\_min}(n_{mot\_k}, SoC_k) \le T_{mot\_k} \le T_{mot\_max}(n_{mot\_k}, SoC_k) \\ T_{d\_k} \cdot \eta_{T\_k} = (T_{e\_k} \cdot i_e + T_{gen\_k} \cdot i_{gen} + T_{mot\_k} \cdot i_{mot}) \cdot i_0 + T_{b\_k} \\ n_{e\_k} = n_{gen\_k} / i_{gen} \text{ if } clutch = 0 \text{ or } 1 \\ n_{e\_k} = n_{mot\_k} / i_{mot} \text{ if } clutch = 1 \end{cases} \tag{14}$$

where $n_e$ and $T_e$ are the engine speed and engine torque, $n_{gen}$ and $T_{gen}$ are the generator speed and generator torque, $n_{mot}$ and $T_{mot}$ are the motor speed and motor torque. $i_e$, $i_{gen}$, $i_{mot}$, and $i_0$ are the engine-main reducing gear ratio, engine - generator gear ratio, motor-main reducing gear ratio, and main reducing gear ratio, respectively. The subscripts *max* and *min* refer to the maximum and minimum limits of each variable.

### B. RANDOM FOREST

The random forest (RF) algorithm is a forest composed of multiple decision trees, which are used to vote to obtain the results of classification. The decision trees add random processes in the row direction and column direction respectively during the generation process. Bootstrapping is used to obtain training data when constructing a decision tree in the row direction. Random sampling without replacement is used in the column direction to obtain the feature subset, and the optimal cut point is obtained accordingly. This is the basic principle of the RF algorithm. Fig. 8 shows the classification principle of the RF algorithm. As can be seen from the figure, the RF is a combined model, and the interior is still based on the decision tree. Unlike a single decision tree classification, the random forest is classified by the voting results of multiple decision trees, and the algorithm is not prone to overfitting problems.

The deduction process of the mapping relationship between energy distribution characteristics and working modes is done by RF model, and off-the-shelf RF model is provided in SPSS Modeler, which is a mature data mining (modeling) software. All we need to do is import the DP results into the model and set the parameters, which we will introduce in Section V.

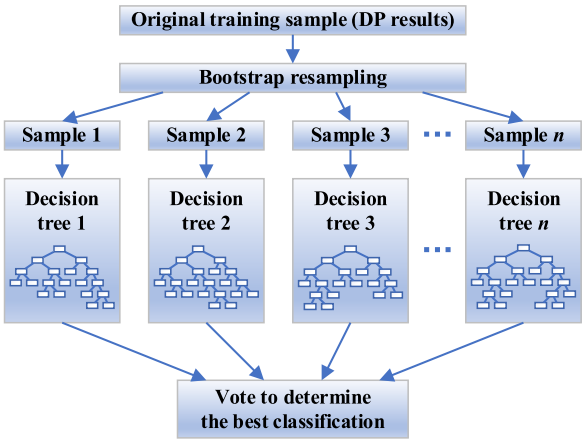


**FIGURE 8.** Random forest sketch.

## IV. POWER DISTRIBUTION STRATEGY DESIGN

This paper introduces a wavelet analysis based on the "Engine optimal operating curve control method". As mentioned in Section II, the sliding resistance coefficients $A_{dyno}$, $B_{dyno}$, and $C_{dyno}$ of the test vehicle are known. It is assumed that the mass of the vehicle is consistent with the mass during the sliding test, and the gradient is 0. Then according to Equation (15), knowing the velocity and acceleration of the vehicle, the power demand of the vehicle $P_d$ of $k$th step can be calculated.

$$P_{d\_k} \cdot \eta_{T\_k} = (A_{dyno} + B_{dyno} \cdot v_k + C_{dyno} \cdot v_k^2 + \delta m \cdot a_k) \cdot v_k \tag{15}$$

If the powertrain needs to enter the Hybrid mode, the steady-state component of the power demand is extracted through wavelet transform and pre-allocated. First, distribute the engine operating points on the minimum fuel consumption curve and try to locate or close to the minimum fuel consumption point. Then, the remaining part of the steady-state power and the transient power is summed and then distributed to the battery. If the battery power cannot meet the requirements, the engine operating point will be adjusted. The improved power distribution process is shown in Fig. 9.

### A. WAVELET TRANSFORM

Wavelet transform (WT) is an ideal tool for signal time-frequency analysis and processing. It inherits and develops the idea of localization of short-time Fourier transform, providing a "time-frequency" window that changes with frequency. There are two types of wavelet transforms, continuous wavelet transform (CWT) and discrete wavelet transform (DWT). In contrast, DWT is more suitable for practical application. However, due to the correlation between the wavelet basis functions of DWT, there will be some overlaps of information. To solve this problem, the multi-resolution analysis (MRA) method is proposed. The basic

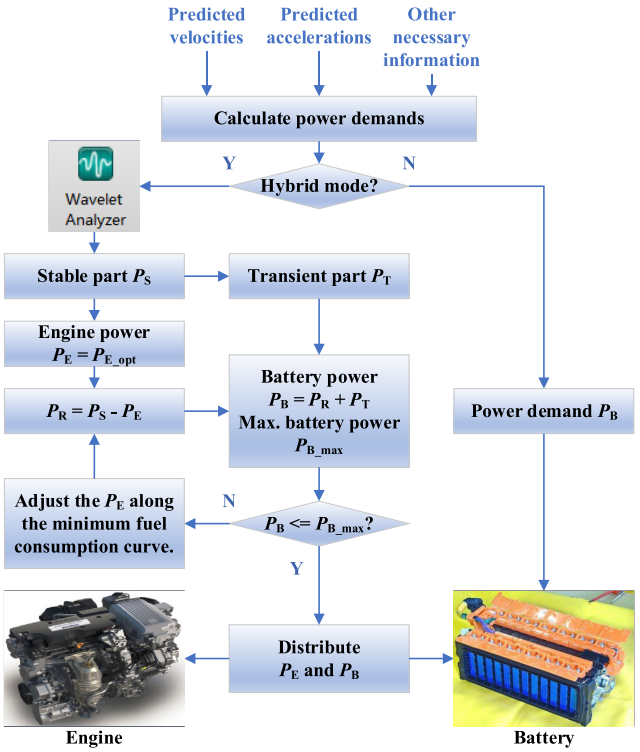


**FIGURE 9.** Power distribution strategy.

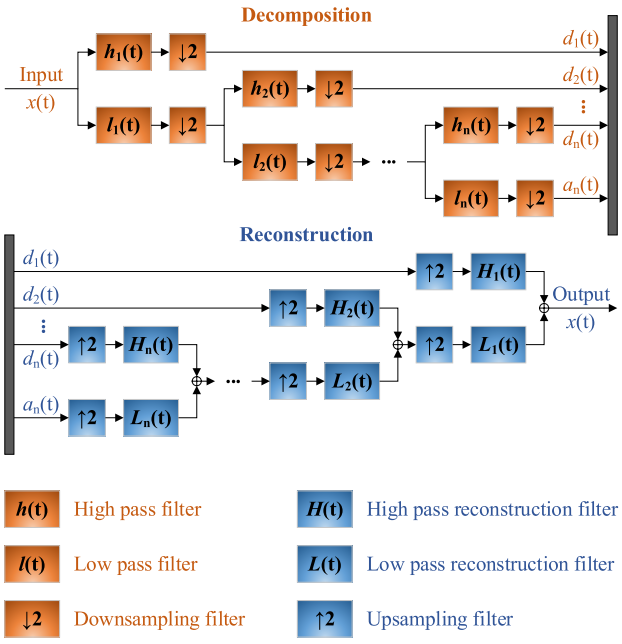


**FIGURE 10.** Basic principle of the Mallat algorithm.

idea of MRA is to process the signal step by step from the macro-level to the micro-level, thereby decomposing a complex signal into multiple simple signals. Based on the theory of MRA, the fast algorithm of wavelet analysis, the Mallat algorithm, is established.

Fig. 10 shows the basic principle of the Mallat algorithm, it is also a general method of WT in practical application. In this paper, the change trajectory of power demand calculated based on Markov velocity prediction is the "Input x(t)" in Fig. 10. And the specific application of WT is to distinguish the steady-state components of power demand from the transient ones after obtaining the power demand change trajectory of a period in the future. The Matlab platform provides the wavelet analysis APP, which can be directly called in the model. As for the specific algorithm of WT, it is not the focus of this paper, so it is not introduced too much.

The signals obtained by transforming different wavelets are also different. Among all wavelets, Haar-WT is more popular due to its simple calculation. The mother wavelet of the Haar-WT can be expressed as:

$$\psi_{Haar}(t) = \begin{cases} 1, & 0 \le t \le \frac{1}{2} \\ -1, & \frac{1}{2} \le t \le 1 \\ 0, & \text{otherwise} \end{cases} \tag{16}$$

### B. IMPROVED MARKOV CHAIN PREDICTION

To make the wavelet transform (WT) distinguish the steady-state components and the transient components in the demand power online, it is necessary to predict the velocity of a period in the future. Due to the "no after effect" characteristic of velocity, Markov Chain (MC) is a good choice to solve this problem. Since the velocity of the $k$th step can be determined by the velocity and acceleration of the $(k-1)$th step, this paper uses the velocity and acceleration as the system state variables for the prediction model of the vehicle velocity.

The accuracy of the prediction results of the traditional first-order Markov model is low. The main reason is that the state transition probability matrix is updated slowly and cannot reflect the characteristics of real driving conditions in time. To obtain prediction results with smaller errors, a high-order Markov prediction model can be used, or the first-order model can be combined with other advanced algorithms, but it will increase the computational complexity and is inconvenient for online implementation. Therefore, the goal of the improvement in this paper is to try not to increase the computational complexity of the algorithm while improving the prediction accuracy. The essence of this improved algorithm is to introduce a prediction result correction function based on the first-order Markov prediction model. The flow chart of the improved Markov prediction algorithm is shown in Fig. 11.

The probability transfer matrix is more like a MAP, where the X-axis and Y-axis are velocity and acceleration, respectively, and the Z-axis is the probability. After inputting the current velocity, we find the X-axis coordinate corresponding to this velocity in the matrix, so that all possible acceleration values and corresponding probability values at this velocity can be obtained. Then, these acceleration values are weighted according to their respective probabilities to obtain a weighted acceleration value, which is the predicted acceleration based on the current velocity. With the current

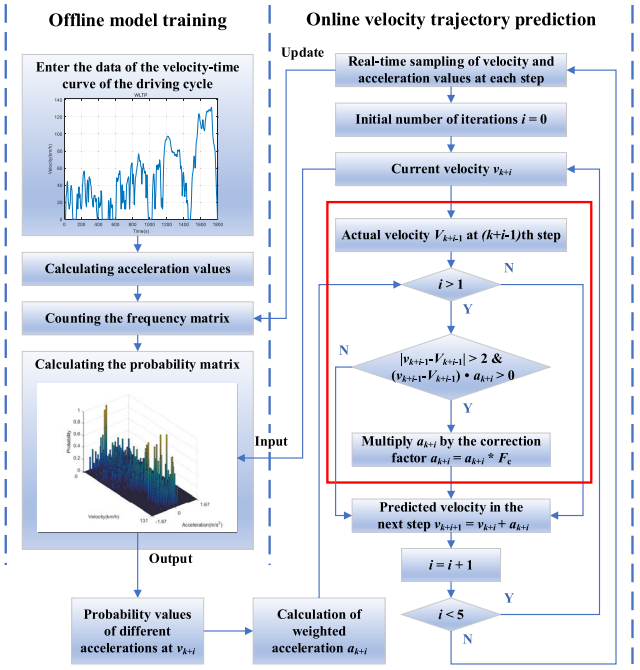


**FIGURE 11.** Improved Markov prediction model.

velocity and the predicted acceleration, the predicted velocity of the next second is obtained.

The classical first-order Markov probability transition matrix is updated slowly, which is difficult to adapt to the complex and changeable actual driving conditions. If the deviation is not corrected in time, it is easy to have a larger and larger prediction deviation. Therefore, the prediction result correction function which is highlighted with a red box in Fig. 11 is added in this paper to improve it. Before predicting the velocity of the next step, we will first check the prediction effect of the last time. If the predicted velocity last time is much higher than the actual one, and the predicted acceleration this time is to continue to accelerate, or the predicted velocity last time is much slower than the actual one, and the predicted acceleration this time continues to decelerate, then the predicted acceleration this time is not appropriate and needs to be revised. If the prediction is acceleration, then we will slow down, if the prediction is deceleration, we will speed up, thus to achieve the effect of inhibiting the prediction error too much and improve the prediction accuracy.

The specific value of the correction factor is determined after we try several different values. It is set to $-1$ because in this case, the final predicted result had the least error from the real value. It is not appropriate to choose this value too large or too small. If it is too small, the improvement effect of prediction error will not be obvious; if it is too large, an overshoot is likely to occur, which will worsen the prediction accuracy.

## V. RESULTS AND DISCUSSION

All the simulations are performed on a laptop computer with 16 GB RAM and a 2.8 GHz of i7 processor. A new driving cycle, namely China Light-duty vehicle Test Cycle-Passenger (CLTC-P) is adopted to perform simulation verification. The velocity-time curve of this cycle is shown in Fig. 12, with a driving distance of 14.48km and driving duration of the 1800s. The initial SoC is set to 50%, and the driving cycle for simulation is 4 consecutive CLTC-P cycles.

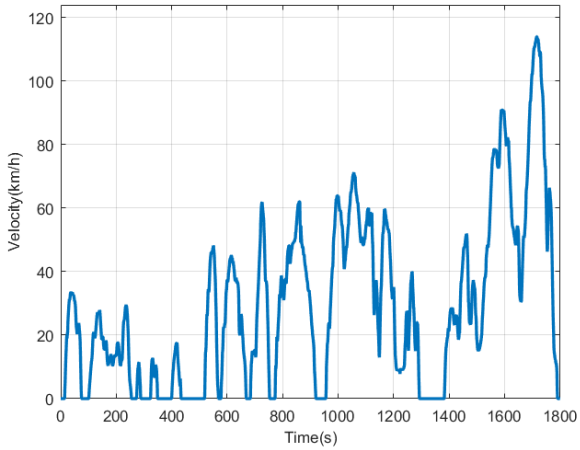


**FIGURE 12.** China Light-duty vehicle Test Cycle-Passenger(CLTC-P).

### A. MODE DIVISION STRATEGY DESIGN

Because the optimality of the working modes division strategy is closely related to the characteristics of the driving cycle and components, it is a critical issue to choose driving cycles to be optimized with DP. The driving cycles selected in this paper are the standard driving cycles that are commonly used in the benchmarking test, including the HWFET cycle, JC08 cycle, NEDC cycle, UDDS cycle, US06 cycle, and WLTP cycle. These cycles are generally obtained by directly extracting some fragments from the actual driving cycles, and then combining them according to certain principles and standards using statistical methods. They can reflect some common features in actual driving conditions. Therefore, the mode division strategy obtained by using these cycles as samples for training DP can have certain generalization performance in theory. Fig. 13 and Fig. 14 shows the velocity-time curves of these standard driving cycles.

At the same time, to obtain more DP optimization results and further enrich the RF samples, this paper also combines the above 6 standard driving cycles in pairs and obtains 36 new driving cycles to run DP to obtain optimization results. Each of these driving cycles is set with 5 different initial SoCs from high to low (100%, 80%, 50%, 30%, 20%). The attribute of each point in the point set contains information such as velocity, vehicle power demand, battery SoC, etc.

With the help of a data mining/modeling software called SPSS Modeler, by connecting modules, importing data, and setting parameters, RF modeling can be easily completed as shown in Fig. 15. The DP optimization result is imported into the RF model via the first module in Fig. 15.

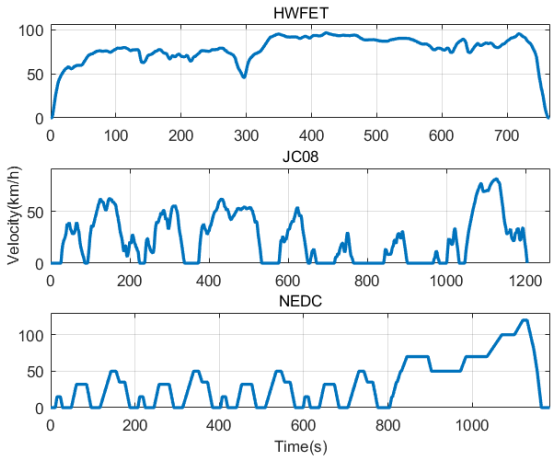


**FIGURE 13.** Standard driving cycles optimized with DP (HWFET JC08 NEDC).

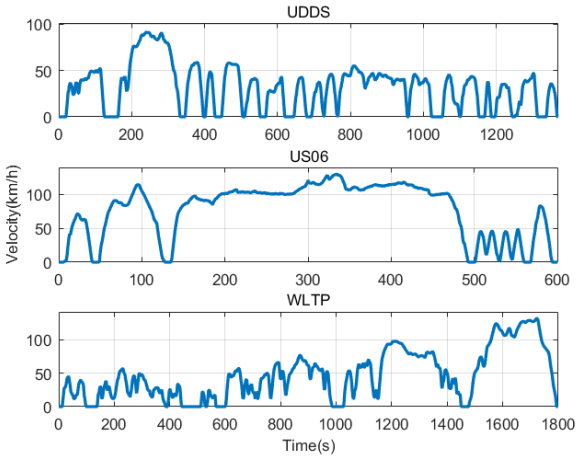


**FIGURE 14.** Standard driving cycles optimized with DP (UDDS US06 WLTP).


**FIGURE 15.** RF model based on SPSS modeler.

The parameter settings are as follows. The predictive variables are velocity, power demand, battery SoC, engine speed, and remaining mileage, and the target is the working mode. The number of decision trees (DT) is 100 and the sample size is 50%. The sample size is the percentage of the number of samples selected each time when constructing DT to the total number of samples. When processing large data sets, reduce the sample size can improve performance. Other parameters are default values.

The rules ranked higher (have obtained more votes from decision trees) in the classification rules are shown in Table 2. The engine speed has become an important reference variable for the division of powertrain working modes. The lowest fuel consumption working point of the engine

**TABLE 2.** The rules ranked higher in the classification rules.

| Number | Decision rules | Corresponding working mode |
|---|---|---|
| 1 | (14.9kW < Power demand ≤ 56.9kW) and (Engine speed ≥ 2540rpm) | Hybrid Drive mode (Battery discharge) |
| 2 | (803rpm < Engine speed ≤ 2540rpm) and (Power demand ≥ 14.9kW) | Hybrid Charge mode (Battery charge) |
| 3 | (Power demand ≤ 27.6kW) and (SoC ≥ 27.9%) and (Engine speed ≤ 2540rpm) | EV mode |

is 120Nm@2500rpm. Combining with the results of RF, when the engine speed is lower than the lowest fuel consumption operating point speed, the powertrain after optimization is more likely to work in EV mode or Hybrid Charge mode. The maximum power of EV mode is also limited. And when the engine speed is higher than the minimum fuel consumption operating point speed, the optimized powertrain tends to work in Hybrid Drive mode.

Moreover, compared with the original control strategy, the Engine mode is excluded from Table 2. This is mainly related to samples of the RF model. The samples of the RF model are derived from DP optimization results for 6 standard driving cycles under different initial SoC values. The maximum velocity of these cycles is not more than 130km/h, and the time of maintaining the maximum velocity is only a few seconds. The Engine mode of the original vehicle is set for the high-speed cruise of the vehicle. In the optimization process, the DP tends to make the engine work in the low-fuel consumption area. In Hybrid mode, there are more such opportunities. However, it is difficult to find the ideal low-fuel consumption working point in Engine mode due to the coupling between engine speed and velocity. Therefore, Engine mode does not appear in the optimization results of DP and is also excluded from Table 2.

### B. MARKOV VELOCITY PREDICTION

To ensure the necessary prediction accuracy and reduce computational complexity, the prediction duration is set to 4 seconds, that is, the trajectory of velocity from $(k+1)$th step to $(k+4)$th step is predicted with the velocity and acceleration of the $k$th step. Then use Equation (15) to calculate the power demand for the next 4 seconds. The correction factor $F_C$ in Fig. 11 is set to $-1$. Fig. 16 and Fig. 17 show the velocity prediction performance before and after improvement, respectively. The driving cycle used to verify the prediction performance is different from the driving cycle used in training the state transition matrix. The WLTP cycle is used to train the state transition matrix, and the CLTC-P cycle is used to verify the performance of velocity prediction. For the new driving cycle, it can be seen that the improved Markov prediction can effectively reduce the impact of the slow update of the state transition matrix, thereby improving the prediction accuracy. The average deviation of the original algorithm

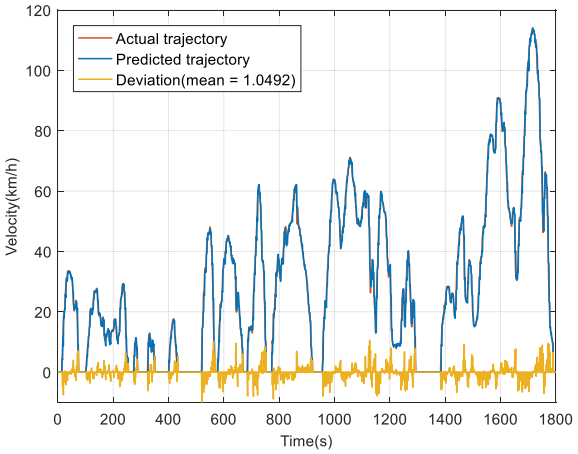


**FIGURE 16.** Original Markov prediction performance.

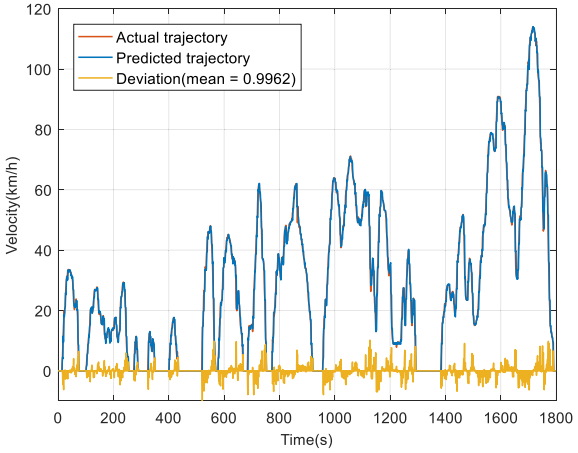


**FIGURE 17.** Improved Markov prediction performance.

is 1.0492km/h. After the improvement, the average deviation is 0.9962km/h, which is 5.3% lower than the original one.

### C. POWER DISTRIBUTION STRATEGY DESIGN

This paper uses a toolkit in Matlab - Wavelet Analyzer to analyze the power demand for a short time in the future. To verify the performance of the power allocation strategy proposed in this paper, the original mode division strategy in the model remains unchanged for the time being. According to the research of the existing literature, considering the accuracy and performance, a WT-based energy management strategy with three decomposition levels is the best choice for PHEV [45]. Therefore, this paper chooses a three-level Harr wavelet to decompose the power demand signal.

Fig. 18 and Fig. 19 are comparisons of the engine start and stop conditions of the two power distribution strategies. It can be seen that compared with the original power distribution strategy, the power distribution strategy proposed in this paper reduces the number of engine starts and stops.

Fig. 20 and Fig. 21 are the engine torque comparisons of the two power distribution strategies. It can be seen

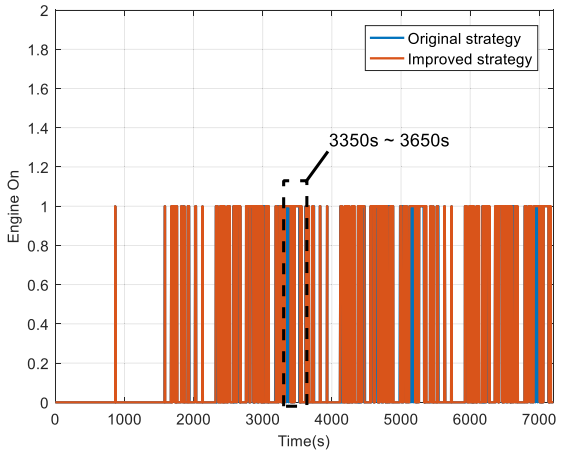


**FIGURE 18.** Comparison of engine start and stop situations.

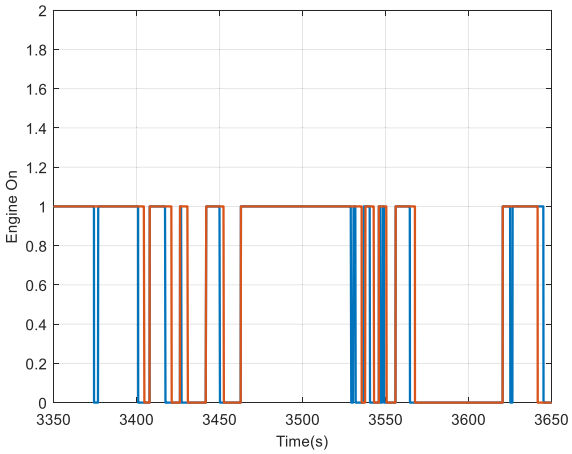


**FIGURE 19.** Comparison of engine start and stop situations (partial).

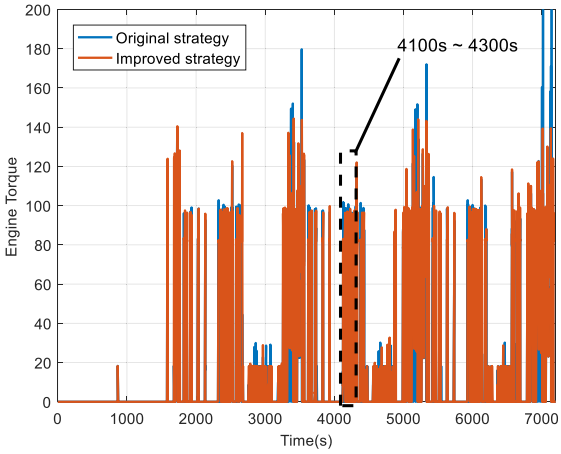


**FIGURE 20.** Comparison of engine torque.

that compared with the original power distribution strategy, the power distribution strategy proposed in this paper effectively reduces the drastic fluctuation of the engine torque.

Fig. 22 and Fig. 23 show the fuel consumption and SoC trajectory comparison of the two power distribution strategies.

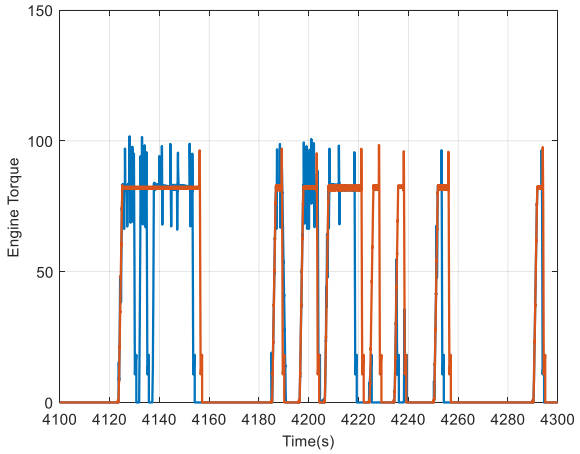


**FIGURE 21.** Comparison of engine torque (partial).

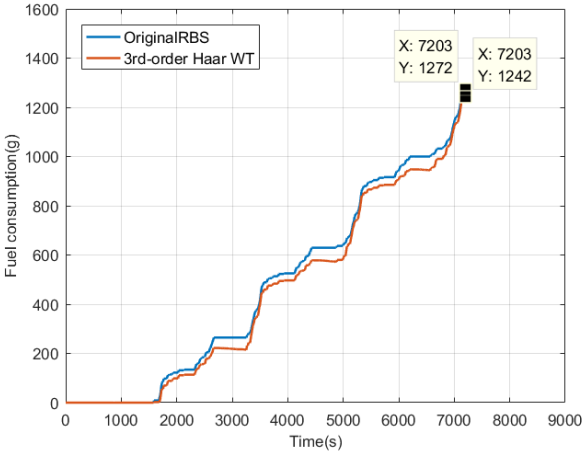


**FIGURE 22.** Comparison of fuel consumption.

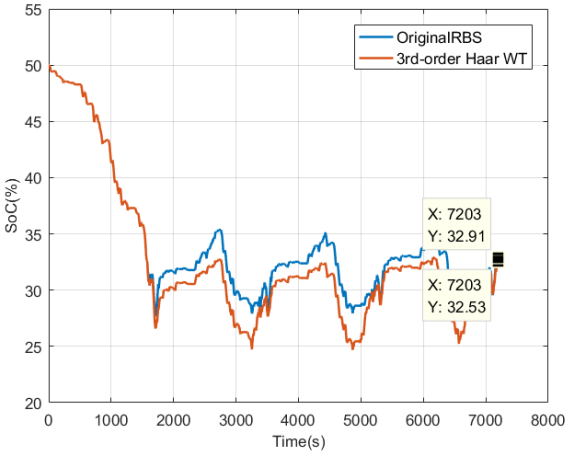


**FIGURE 23.** Comparison of SoC trajectories.

The improved power distribution strategy reduces the number of starts and stops of the engine and the sharp fluctuation of torque. The PHEV consumes 1272g gasoline after four consecutive CLTC-P cycles under the original-rule-based control. After the power distribution strategy is improved, the fuel consumption is 1242g, a decrease of 2.36% compared with the original. Of course, as shown in Fig. 19, due to the reduction of transient components in engine torque, the motor has to provide more driving torque, which in turn leads to an increase in electricity consumption. The terminal SoC of the original strategy is 32.91%. Considering that the initial SoC is 50%, so the $\Delta SoC$ is 17.09%. While the terminal SoC of the improved power distribution strategy is 32.53%, so the $\Delta SoC$ is 17.47%. The electricity consumption is increased by 2.22%.

### D. ENERGY MANAGEMENT STRATEGY VERIFICATION

The Energy Management Strategy (EMS) proposed in this paper is composed of the mode division strategy obtained by the random forest algorithm, and the power distribution strategy improved by using Markov prediction and wavelet analysis. This section will verify the control effect of the EMS proposed. The driving cycle used for verification is still four consecutive CLTC-P cycles. The initial SoC is set to 50%.

The SoC trajectory and fuel consumption for four consecutive driving cycles before the EMS is improved are shown in Fig. 24. The PHEV consumed 1272g gasoline after four driving cycles under the original-rule-based control. The trip distance is 57.9km, so the fuel consumption per 100 km is 3.14L/100km. The powertrain switches to CS state from CD state at about 1700s of the trip, and the terminal SOC value is 32.91%.

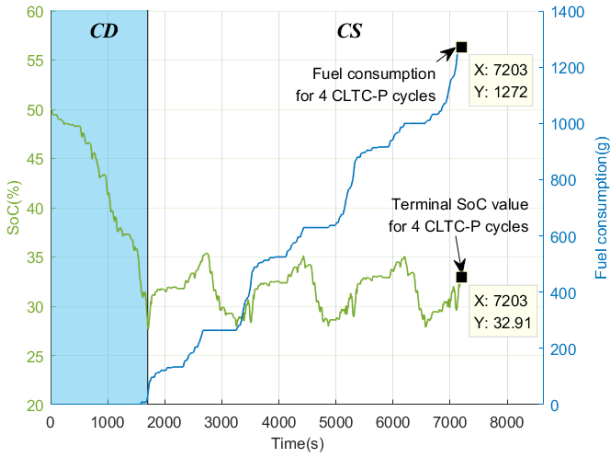


**FIGURE 24.** SoC trajectory and fuel consumption (Original EMS).

After the mode division strategy is improved, the SoC trajectory and fuel consumption for the same driving cycles are shown in Fig. 25, and the initial SOC is also set to 50%. The powertrain switches to CS state from CD state at about 2400s, which means that the improved strategy works longer in CD state, and the SoC decline rate is also slower. The final fuel consumption of the PHEV is 1165g, which is 2.88L/100km after conversion. So the fuel consumption per 100 km decreased by 8.28%, while electricity consumption is increased by 4.04%.

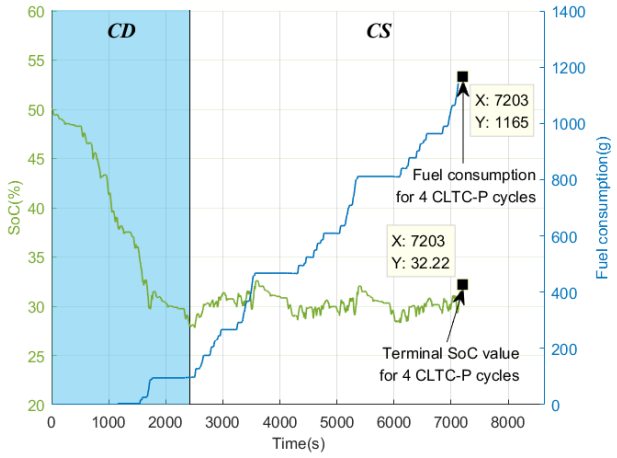


**FIGURE 25.** SoC trajectory and fuel consumption (Improved EMS).

To facilitate comparison, the comparison of SoC trajectories under different strategies is shown in Fig. 26 and the comparison results of different strategies are listed in Table 3. The fuel consumption of four consecutive CLTC-P cycles under DP control is 2.33L/100km, and the terminal SoC value is 33.2%.

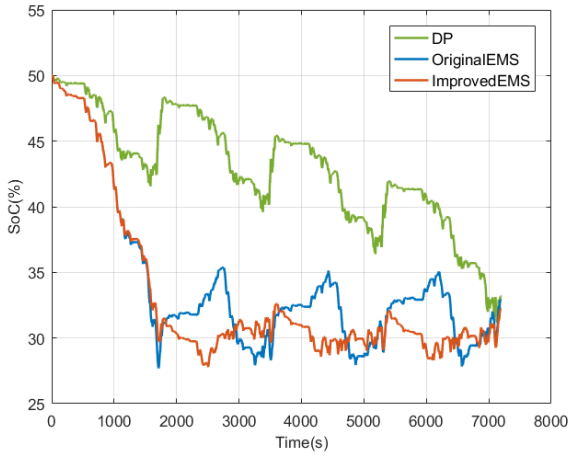


**FIGURE 26.** Comparison of SoC trajectories.

**TABLE 3.** Energy consumption under different control strategies.

| Control strategy | Original EMS | Improved EMS | DP |
|---|---|---|---|
| Fuel consumption(L/100 km) | 3.14 | 2.88 | 2.33 |
| Initial SoC(%) | 50 | 50 | 50 |
| Terminal SoC(%) | 32.91 | 32.22 | 33.2 |
| ΔSoC(%) | 17.09 | 17.78 | 16.8 |

In Fig. 26, the SoC trajectories of the original strategy and the improved strategy are the same before the 1200s, while significant differences appear after the 1200s. The reason for this phenomenon is mainly due to the limitations of rule-based strategies. The optimization strategy in this paper is essentially a rule-based control strategy, which is divided into charge depleting (CD) and charge sustaining (CS) status. Under the condition of sufficient electricity, it will give priority to electricity consumption, so the control effect is certainly not as significant as A-ECMS, MPC, and other real-time optimization strategies. Although the fuel economy has been improved compared with the original strategy, there is still room for improvement in our optimization strategy compared with the control effect of DP.

According to the bench-marking test results, the maximum velocity of pure electric mode in the original strategy is 100km/h(CD) and 70km/h(CS). Therefore, the powertrain has to start the engine and combine the clutch when velocity is high, to meet high-speed driving requirements. Therefore, as shown in Fig. 27, the powertrain has to enter Engine mode. This setting of the original vehicle mainly takes into account the high-speed cruising condition. If the vehicle enters Engine mode in high-speed cruising conditions, it is directly driven by the engine, and the engine speed and the velocity are not decoupled. But due to the high engine speed, the engine can still work with lower fuel consumption, so the fuel consumption performance is still satisfactory. Besides, the battery power can also be released to prepare for the power demand during high-speed acceleration.

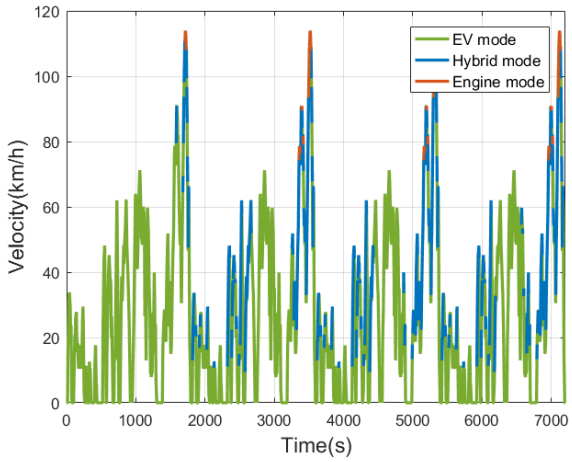


**FIGURE 27.** Mode selection (Original EMS).

For the new strategy, since the velocity of the driving cycles selected for DP optimization are not very high, the powertrain working in the Hybrid mode can fully meet the driving requirements. At the same time, due to the decoupling of velocity and engine speed, the engine working point can be adjusted freely, so the fuel economy is better. Although there is a second conversion of energy when the powertrain works in Hybrid mode, the parameters matching of components of the vehicle are good. When the engine works in the low fuel consumption area, the generator also happens to work in the high-efficiency area, so the energy loss is not too much. Therefore, based on the above two reasons, in the high-speed section of the driving cycle, the powertrain does not need to switch to Engine mode, as shown in Fig. 28.

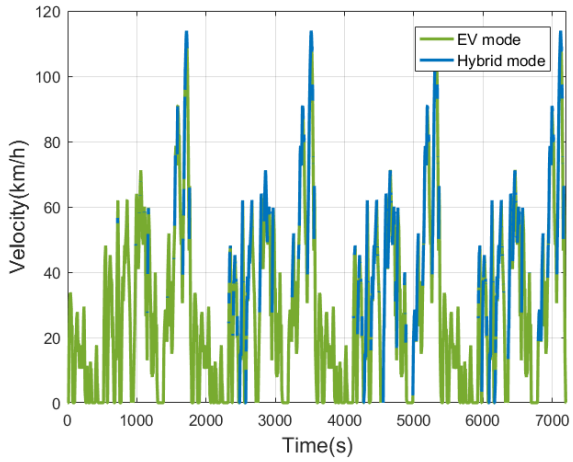


**FIGURE 28.** Mode selection (Improved EMS).

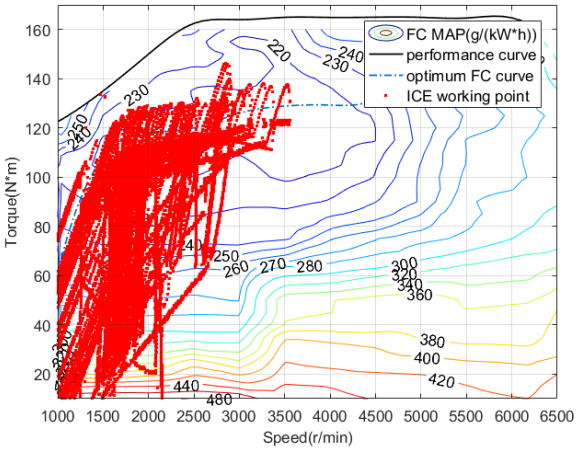


**FIGURE 29.** Engine working points distribution (Original EMS).

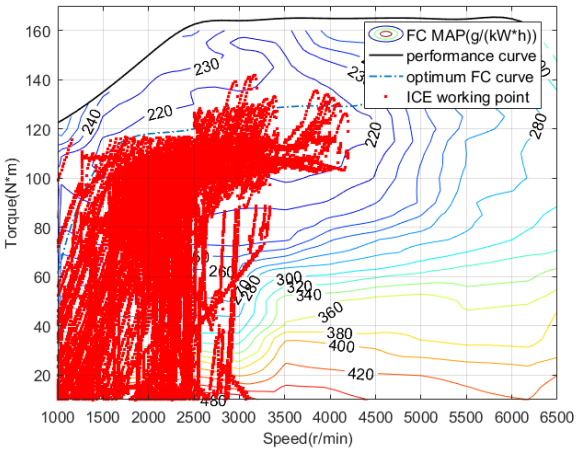


**FIGURE 30.** Engine working points distribution (Improved EMS).

Fig. 29 and Fig. 30 are the engine operating point distribution of the two strategies. Compared with the original EMS, there are more engine working points distributed in the low fuel consumption area near the optimal fuel consumption curve under the control of the improved EMS. Therefore, the fuel consumption performance of improved EMS is better, as shown in Table 3. The fuel consumption per 100 km under the control of the new energy management strategy is decreased by 8.28%, while electricity consumption is increased by 4.04%.

## VI. CONCLUSION

This paper introduces an EMS design method for a PHEV based on the data-driven approach and online signal analysis. It includes two parts, mode division strategy design, and power distribution strategy design. Using the RF in data mining technology to analyze optimization results of DP can quickly extract key information and establish optimal and understandable mode division strategy with high precision and stability directly. Besides, integrating the classic "Engine optimal operating curve control" strategy with WT and Markov prediction, which not only enhances the adaptability of the strategy to different driving conditions but also improves the fuel economy by reducing the impact of transient power on the engine operation. At the same time, to improve the prediction accuracy of the algorithm without increasing the computational complexity, this paper adds a prediction result correction function to the first-order Markov prediction model to reduce the impact of slow update of the probability matrix on prediction accuracy. The simulation results show the average prediction error of the improved Markov prediction model is reduced by 5.3%. And compared with the original strategy, the improved strategy reduces fuel consumption by 8.28%, while electricity consumption is increased by 4.04% during four consecutive CLTC-P cycles. Therefore, the proposed EMS design method can provide a theoretical reference for the extraction rules in engineering practice.

Future work will mainly focus on the following aspects. The first one is to compare our strategy with other RBSs optimized by different optimization algorithms. The second one is to further improve the strategy in this paper. Perhaps an adaptive mode division strategy based on driving conditions recognition is a better approach. And the last one is performing HIL simulation to verify control function and fuel-saving effect in a real-time environment.

## ACKNOWLEDGMENT

The authors would like to express their gratitude to the reviewers of the manuscript for their valuable suggestions and comments.

## REFERENCES

[1] G. Jinquan, H. Hongwen, P. Jiankun, and Z. Nana, "A novel MPC-based adaptive energy management strategy in plug-in hybrid electric vehicles," *Energy*, vol. 175, pp. 378–392, May 2019.

[2] H. Guo, D. Hou, S. Du, L. Zhao, J. Wu, and N. Yan, "A driving pattern recognition-based energy management for plug-in hybrid electric bus to counter the noise of stochastic vehicle mass," *Energy*, vol. 198, Mar. 2020, Art. no. 117289.

[3] H. Guo, S. Lu, H. Hui, C. Bao, and J. Shangguan, "Receding horizon control-based energy management for plug-in hybrid electric buses using a predictive model of terminal SOC constraint in consideration of stochastic vehicle mass," *Energy*, vol. 176, pp. 292–308, Jun. 2019.

[4] S.-Y. Chen, C.-H. Wu, Y.-H. Hung, and C.-T. Chung, "Optimal strategies of energy management integrated with transmission control for a hybrid electric vehicle using dynamic particle swarm optimization," *Energy*, vol. 160, pp. 154–170, Oct. 2018.
[5] J. Hu, D. Liu, C. Du, F. Yan, and C. Lv, "Intelligent energy management strategy of hybrid energy storage system for electric vehicle based on driving pattern recognition," *Energy*, vol. 198, Mar. 2020, Art. no. 117298.
[6] R. Koubaa, S. Bacha, M. Smaoui, and L. Krichen, "Robust optimization based energy management of a fuel cell/ultra-capacitor hybrid electric vehicle under uncertainty," *Energy*, vol. 200, Apr. 2020, Art. no. 117530.
[7] R. Bagwe, A. Byerly, E. C. dos Santos, and Z. Ben-Miled, "Adaptive rule-based energy management strategy for a parallel HEV," *Energies*, vol. 12, no. 23, p. 4472, 2019.
[8] J. Cao and R. Xiong, "Reinforcement learning-based real-time energy management for plug-in hybrid electric vehicle with hybrid energy storage system," *Energy Procedia*, vol. 142, pp. 1896–1901, Dec. 2017.
[9] Y. Yang, Y. Zhang, J. Tian, and T. Li, "Adaptive real-time optimal energy management strategy for extender range electric vehicle," *Energy*, vol. 197, Feb. 2020, Art. no. 117237.
[10] J. Shangguan, H. Guo, and M. Yue, "Robust energy management of plug-in hybrid electric bus considering the uncertainties of driving cycles and vehicle mass," *Energy*, vol. 203, May 2020, Art. no. 117836, doi: 10.1016/j.energy.2020.117836.
[11] H. Jiang, L. Xu, J. Li, Z. Hu, and M. Ouyang, "Energy management and component sizing for a fuel cell/battery/supercapacitor hybrid powertrain based on two-dimensional optimization algorithms," *Energy*, vol. 177, pp. 386–396, Jun. 2019.
[12] M. Sellali, A. Betka, S. Drid, A. Djerdir, L. Allaoui, and M. Tiar, "Novel control implementation for electric vehicles based on fuzzy -back stepping approach," *Energy*, vol. 178, pp. 644–655, Jul. 2019.
[13] Z. Fu, L. Zhu, F. Tao, P. Si, and L. Sun, "Optimization based energy management strategy for fuel cell/battery/ultracapacitor hybrid vehicle considering fuel economy and fuel cell lifespan," *Int. J. Hydrogen Energy*, vol. 45, no. 15, pp. 8875–8886, Mar. 2020.
[14] H. Liu, X. Li, W. Wang, L. Han, and C. Xiang, "Markov velocity predictor and radial basis function neural network-based real-time energy management strategy for plug-in hybrid electric vehicles," *Energy*, vol. 152, pp. 427–444, Jun. 2018.
[15] J. Peng, H. He, and R. Xiong, "Rule based energy management strategy for a series–parallel plug-in hybrid electric bus optimized by dynamic programming," *Appl. Energy*, vol. 185, pp. 1633–1643, Jan. 2017.
[16] Z. Lei, D. Qin, L. Hou, J. Peng, Y. Liu, and Z. Chen, "An adaptive equivalent consumption minimization strategy for plug-in hybrid electric vehicles based on traffic information," *Energy*, vol. 190, Jan. 2020, Art. no. 116409.
[17] Y. Wang, X. Zeng, D. Song, and N. Yang, "Optimal rule design methodology for energy management strategy of a power-split hybrid electric bus," *Energy*, vol. 185, pp. 1086–1099, Oct. 2019.
[18] H. Zhou, Z. Xu, L. Liu, D. Liu, and L. Zhang, "A rule-based energy management strategy based on dynamic programming for hydraulic hybrid vehicles," *Math. Problems Eng.*, vol. 2018, pp. 1–10, Oct. 2018.
[19] R. Bellman, "Dynamic programming and Lagrange multipliers," *Proc. Nat. Acad. Sci. USA*, vol. 42, no. 10, pp. 767–769, Oct. 1956.
[20] A. M. Ali, A. Ghanbar, and D. Soffker, "Optimal control of multi-source electric vehicles in real time using advisory dynamic programming," *IEEE Trans. Veh. Technol.*, vol. 68, no. 11, pp. 10394–10405, Nov. 2019.
[21] C. Xiang, F. Ding, W. Wang, and W. He, "Energy management of a dual-mode power-split hybrid electric vehicle based on velocity prediction and nonlinear model predictive control," *Appl. Energy*, vol. 189, pp. 640–653, Mar. 2017.
[22] Y. Yang, H. Pei, X. Hu, Y. Liu, C. Hou, and D. Cao, "Fuel economy optimization of power split hybrid vehicles: A rapid dynamic programming approach," *Energy*, vol. 166, pp. 929–938, Jan. 2019.
[23] W. Geng, D. Lou, C. Wang, and T. Zhang, "A cascaded energy management optimization method of multimode power-split hybrid electric vehicles," *Energy*, vol. 199, May 2020, Art. no. 117224.
[24] B. Ma, D. Wang, S. Cheng, and X. Xie, "Modeling and analysis for vertical handoff based on the decision tree in a heterogeneous vehicle network," *IEEE Access*, vol. 5, pp. 8812–8824, 2017.
[25] H. A. Yavasoglu, Y. E. Tetik, and K. Gokce, "Implementation of machine learning based real time range estimation method without destination knowledge for BEVs," *Energy*, vol. 172, pp. 1179–1186, Apr. 2019.
[26] L. Breiman, "Random forests," *Mach. Learn.*, vol. 45, no. 1, pp. 5–32, 2001.
[27] Y. Lu, Y. Li, D. Xie, E. Wei, X. Bao, H. Chen, and X. Zhong, "The application of improved random forest algorithm on the prediction of electric vehicle charging load," *Energies*, vol. 11, no. 11, p. 3207, Nov. 2018.
[28] P. Thanh Noi and M. Kappas, "Comparison of random forest, k-Nearest neighbor, and support vector machine classifiers for land cover classification using Sentinel-2 imagery," *Sensors*, vol. 18, no. 2, p. 18, Dec. 2017.
[29] W. Chen, S. Zhang, R. Li, and H. Shahabi, "Performance evaluation of the GIS-based data mining techniques of best-first decision tree, random forest, and naïve bayes tree for landslide susceptibility modeling," *Sci. Total Environ.*, vol. 644, pp. 1006–1018, Dec. 2018.
[30] D. Zhang, L. Qian, B. Mao, C. Huang, B. Huang, and Y. Si, "A data-driven design for fault detection of wind turbines using random forests and XGboost," *IEEE Access*, vol. 6, pp. 21020–21031, 2018.
[31] L. Wu, Y. Ci, Y. Wang, and P. Chen, "Fuel consumption at the oversaturated signalized intersection considering queue effects: A case study in Harbin, China," *Energy*, vol. 192, Feb. 2020, Art. no. 116654.
[32] X. Tang, D. Zhang, T. Liu, A. Khajepour, H. Yu, and H. Wang, "Research on the energy control of a dual-motor hybrid vehicle during engine start-stop process," *Energy*, vol. 166, pp. 1181–1193, Jan. 2019.
[33] Y. Cai, L. Yang, Z. Deng, X. Zhao, and H. Deng, "Online identification of lithium-ion battery state-of-health based on fast wavelet transform and cross D-Markov machine," *Energy*, vol. 147, pp. 621–635, Mar. 2018.
[34] X. Zhang, C. C. Mi, A. Masrur, and D. Daniszewski, "Wavelet-transform-based power management of hybrid vehicles with multiple on-board energy sources including fuel cell, battery and ultracapacitor," *J. Power Sources*, vol. 185, no. 2, pp. 1533–1543, Dec. 2008.
[35] M. Yan, M. Li, H. He, J. Peng, and C. Sun, "Rule-based energy management for dual-source electric buses extracted by wavelet transform," *J. Cleaner Prod.*, vol. 189, pp. 116–127, Jul. 2018.
[36] Z. Li, A. Khajepour, and J. Song, "A comprehensive review of the key technologies for pure electric vehicles," *Energy*, vol. 182, pp. 824–839, Sep. 2019.
[37] G. Li, Z. Yang, B. Li, and H. Bi, "Power allocation smoothing strategy for hybrid energy storage system based on Markov decision process," *Appl. Energy*, vol. 241, pp. 152–163, May 2019.
[38] J. Shin and M. Sunwoo, "Vehicle speed prediction using a Markov chain with speed constraints," *IEEE Trans. Intell. Transp. Syst.*, vol. 20, no. 9, pp. 3201–3211, Sep. 2019.
[39] S. Dong, D. Liu, R. Ouyang, Y. Zhu, L. Li, T. Li, and J. Liu, "Second-order Markov assumption based bayes classifier for networked data with heterophily," *IEEE Access*, vol. 7, pp. 34153–34161, 2019.
[40] H. Xiong and R. Mamon, "A higher-order Markov chain-modulated model for electricity spot-price dynamics," *Appl. Energy*, vols. 233–234, pp. 495–515, Jan. 2019.
[41] Y. Zhou, A. Ravey, and M. Péra, "Multi-mode predictive energy management for fuel cell hybrid electric vehicles using Markov driving pattern recognizer," *Appl. Energy*, vol. 258, Jan. 2020, Art. no. 114057.
[42] T. Liu, B. Wang, and C. Yang, "Online Markov chain-based energy management for a hybrid tracked vehicle with speedy Q-learning," *Energy*, vol. 160, pp. 544–555, Oct. 2018.
[43] Y. Iwafune, K. Ogimoto, Y. Kobayashi, and K. Murai, "Driving simulator for electric vehicles using the Markov chain Monte Carlo method and evaluation of the demand response effect in residential houses," *IEEE Access*, vol. 8, pp. 47654–47663, 2020.
[44] J. Liu, Y. Chen, W. Li, F. Shang, and J. Zhan, "Hybrid-trip-model-based energy management of a PHEV with computation-optimized dynamic programming," *IEEE Trans. Veh. Technol.*, vol. 67, no. 1, pp. 338–353, Jan. 2018.
[45] C. Wang, R. Xiong, H. He, Y. Zhang, and W. Shen, "Comparison of decomposition levels for wavelet transform based energy management in a plug-in hybrid electric vehicle," *J. Cleaner Prod.*, vol. 210, pp. 1085–1097, Feb. 2019.

**JIANAN ZHANG** received the B.S. degree from the College of Automotive Engineering, Jilin University, Changchun, China, in 2015, where he is currently pursuing the Ph.D. degree.

His research interests include the energy management theory and working condition adaptive technology.

**LIANG CHU** received the Ph.D. degree from the College of Automotive Engineering, Jilin University, Changchun, China, in 2000.

He is currently with Jilin University, as a Professor and a Ph.D. Supervisor. His research interests include braking energy recovery technology, energy management theory and working condition adaptive technology, new electric drive systems, and assisted driving technology.

**CHONG GUO** received the Ph.D. degree from the College of Automotive Engineering, Jilin University, Changchun, China, in 2016.

He is currently a Lecturer with Jilin University. His research interests include energy management theory and working condition adaptive technology, new electric drive systems, and assisted driving technology.

**ZICHENG FU** received the M.S. degree from the School of Automobile, Chang'an University, Xi'an, China, in 2012. He is currently pursuing the Ph.D. degree with the College of Automotive Engineering, Jilin University.

His research interests include the energy management theory and working condition adaptive technology.

**DI ZHAO** received the B.S. degree from the College of Automotive Engineering, Jilin University, Changchun, China, in 2012, where he is currently pursuing the Ph.D. degree.

His research interests include the braking energy recovery technology and assisted driving technology.